# Rapid #: -20915716

CROSS REF ID: **560622**

LENDER: **CUV (Univ. of California, Davis) :: Shields Library**

BORROWER: **TEU (Temple University) :: Main Library**

| | |
|---|---|
| TYPE: | Article CC:CCL |
| JOURNAL TITLE: | Computer aided geometric design |
| USER JOURNAL TITLE: | Computer aided geometric design |
| ARTICLE TITLE: | Analysis and applications of pipe surfaces |
| ARTICLE AUTHOR: | Maekawa, Takashi |
| VOLUME: | 15 |
| ISSUE: | 5 |
| MONTH: | |
| YEAR: | 1998 |
| PAGES: | 437-458 |
| ISSN: | 0167-8396 |
| OCLC #: | 38840689 |

Processed by RapidX: 6/20/2023 2:16:39 PM

ELSEVIER

Computer Aided Geometric Design 15 (1998) 437–458

COMPUTER AIDED GEOMETRIC DESIGN

# Analysis and applications of pipe surfaces

Takashi Maekawa [a,*], Nicholas M. Patrikalakis [a], Takis Sakkalis [b], Guoxin Yu [a]

[a] *Massachusetts Institute of Technology, Department of Ocean Engineering, Design Laboratory, Cambridge, MA 02139-4307, USA*

[b] *Agricultural University of Athens, Department of Mathematics, 118 55 Athens, Greece*

Received January 1997; revised July 1997

**Abstract**

A pipe (or tubular) surface is the envelope of a one-parameter family of spheres with constant radii $r$ and centers $\mathbf{C}(t)$. In this paper we investigate necessary and sufficient conditions for the nonsingularity of pipe surfaces. In addition, when $\mathbf{C}(t)$ is a rational function, we develop an algorithmic method for the rational parametrization of such a surface. The latter is based on finding two rational functions $\alpha(t)$ and $\beta(t)$ such that $|\mathbf{C}'(t)|^2 = \alpha^2(t) + \beta^2(t)$ (Lü and Pottmann, 1996).


*Keywords:* Pipe surface; Local self-intersection; Global self-intersection; Rational parametrization

## 1. Introduction

Pipe surfaces were first introduced by Monge (1850) and defined as follows: Given a space curve $\mathbf{C}(t)$ and a positive number $r$, the *pipe* surface with *spine* curve $\mathbf{C}(t)$ is defined to be the envelope of the set of spheres with radius $r$ which are centered at $\mathbf{C}(t)$. For simplicity, we will denote such a surface by $\mathbf{P}_C(r)$. Pipe surfaces have many practical applications, such as in shape reconstruction (Shani and Ballard, 1984), construction of blending surfaces (Pegna and Wilde, 1990; Farouki and Sverrisson, 1996), transition surfaces between pipes (Pegna and Wilde, 1990), and in robotic path planning (Wang and Blackmore,

* Corresponding author.

0167-8396/98/$19.00 
*PII* S0167-8396(97)00042-3

1997). They also have theoretical applications as well; for example, do Carmo uses them in the proof of two very important theorems in Differential Geometry concerning the total curvature of simple space curves (do Carmo, 1976, pp. 399–402).

If we assume that the spine curve $\mathbf{C}(t)$ is regular, i.e., $\mathbf{C}(t)$ is simple and $|\mathbf{C}'(t)| \neq 0$, there exist two kinds of singularities on pipe surfaces: those that arise from local differential geometry properties of the surface and those that come from global distance properties of the surface. The first type of singularity occurs when the radius of the pipe surface $r$ exceeds the minimum radius of curvature of the spine curve; we refer to this singularity as *local self-intersection*. The second one happens, for example, when twice the radius $r$ of the pipe surface is larger than the minimum distance between two interior points (excluding the two end points) on the spine curve; we refer to this singularity as *global self-intersection*. Kreyszig (1959), do Carmo (1976) and Rossignac (1985) derive the condition for local self-intersection of a pipe surface and Shani and Ballard (1984) describe a method to prevent local self-intersection of a generalized cylinder. However, to the best of our knowledge, there is no literature which deals with the question of global self-intersection of a pipe surface.

Lü and Pottmann (1996) proved the surprising result that a pipe surface whose spine curve $\mathbf{C}(t)$ is rational can be rationally parametrized. The key to their method is the decomposition of a nonnegative rational function into the sum of the squares of two rational functions. However, this problem remains unsolved from the algorithmic point of view.

In this paper we will be concerned first with the question of when a pipe surface is nonsingular. More precisely, given a regular space curve $\mathbf{C}(t)$ we will find the maximum $R$, $R > 0$, so that the pipe surface $\mathbf{P}_C(r)$ is nonsingular, whenever $r < R$. Our second point will be the development of an algorithm to decompose a nonnegative rational function into the sum of the squares of two rational functions. Using this decomposition we will then find a rational parametrization of the pipe surface following the method of (Lü and Pottmann, 1996).

One immediate application of our ideas lies in the area of finding a topologically reliable approximation of a space curve (Cho et al., 1996). More precisely, suppose we are given a regular space curve $\mathbf{C}(t)$, and would like to approximate $\mathbf{C}(t)$ with another curve $\mathbf{K}(t)$—within a prescribed tolerance—in a natural way; that is, there is a *space* homeomorphism $h : \mathbb{R}^3 \to \mathbb{R}^3$ that carries $\mathbf{C}(t)$ onto $\mathbf{K}(t)$. One important consequence of such a homeomorphism is that $\mathbf{C}(t)$ and $\mathbf{K}(t)$ have the same *knot* type. To do this, we first construct a nonsingular pipe surface $\mathbf{P}_C(r)$. Then, we construct a curve $\mathbf{K}(t)$ that lies inside $\mathbf{P}_C(r)$, and "looks like" $\mathbf{C}(t)$ (see Section 6). By taking $r$ to be the tolerance we have a reliable approximation of the given curve.

The paper is organized as follows: Section 2 presents the question of local self-intersection of the pipe surface, while Section 3 deals with the problem of global self-intersection. An algorithm to decompose a nonnegative rational function into the sum of the squares of two rational functions is developed in Section 4. Illustrative examples are presented in Section 5. Section 6 discusses the application of pipe surfaces in topologically reliable approximation of space curves, and concluding remarks are provided in Section 7.

## 2. Local self-intersection

The pipe surface $\mathbf{P}_C(r)$ can be parametrized using the Frenet trihedron $(\mathbf{t}(t), \mathbf{n}(t), \mathbf{b}(t))$ (do Carmo, 1976; Rossignac, 1985) as follows:

$$\mathbf{P}(t,\theta) = \mathbf{C}(t) + r\big(\cos\theta\,\mathbf{n}(t) + \sin\theta\,\mathbf{b}(t)\big), \tag{1}$$

where $t \in [0,1]$ and $\theta \in [0, 2\pi]$. Its partial derivative with respect to $t$ is given by

$$\mathbf{P}_t(t,\theta) = \mathbf{C}'(t) + r\big(\cos\theta\,\mathbf{n}'(t) + \sin\theta\,\mathbf{b}'(t)\big). \tag{2}$$

Eq. (2) can be rewritten using the Frenet formulae as

$$\mathbf{P}_t(t,\theta) = \big|\mathbf{C}'(t)\big|\big(1 - \kappa(t)r\cos\theta\big)\mathbf{t} - r\big|\mathbf{C}'(t)\big|\sin\theta\tau(t)\mathbf{n} + r\big|\mathbf{C}'(t)\big|\cos\theta\tau\,\mathbf{b}. \tag{3}$$

where $\kappa(t)$ and $\tau(t)$ are the curvature and torsion of the spine curve. Similarly we can derive $\mathbf{P}_\theta$ as

$$\mathbf{P}_\theta(t,\theta) = r\big(-\sin\theta\,\mathbf{n}(t) + \cos\theta\,\mathbf{b}(t)\big). \tag{4}$$

The surface normal of the pipe surface can be obtained by taking the cross product of equations (3) and (4) yielding

$$\mathbf{P}_t \times \mathbf{P}_\theta = -|\mathbf{C}'(t)|r\big(1 - \kappa(t)r\cos\theta\big)\big(\sin\theta\,\mathbf{b}(t) + \cos\theta\,\mathbf{n}(t)\big). \tag{5}$$

It is easy to observe (Kreyszig, 1959; do Carmo, 1976; Rossignac, 1985) that the pipe surface becomes singular when $1 - \kappa(t)r\cos\theta = 0$. Since $\cos\theta$ varies between $-1$ and 1, there will be no local self-intersection if $\kappa(t)r < 1$. Therefore, to avoid local self-intersection we need to find the largest curvature $\kappa_{\max}$ of the spine curve and set the radius of the pipe surface such that $r < 1/\kappa_{\max}$.

The curvature $\kappa(t)$ of a space curve $\mathbf{C}(t)$, is given by

$$\kappa(t) = \frac{|\mathbf{C}'(t) \times \mathbf{C}''(t)|}{|\mathbf{C}'(t)|^3}. \tag{6}$$

Thus, to find the largest curvature $\kappa_{\max}$ we need to locate the critical points of $\kappa(t)$, i.e., solve the equation $\kappa'(t) = 0$, and decide whether they are local maxima. Then we compare these local maxima with the curvature at the end points, i.e., $\kappa(0)$ and $\kappa(1)$, and obtain the global largest curvature. This problem can be solved by elementary calculus. If the spine curve is given by a rational Bézier curve, equation $\kappa'(t) = 0$ reduces to a single univariate nonlinear polynomial equation. In the case where the spine curve is a rational B-spline, we can extract the rational Bézier segments by knot insertion (Hoschek and Lasser, 1993). Cho et al. (1996) describe in detail how to obtain $\kappa'(t) = 0$ for integral Bézier curves.

## 3. Global self-intersection

In this section we will consider how to find the maximum possible radius of the pipe surface such that it will not self-intersect in a global manner. The global self-intersection can further be divided into three cases.

(1) *End circle to end circle*: Two end circles of the pipe surface touch each other.
(2) *Body to body*: Two different body portions of the pipe surface touch each other.
(3) *End circle to body*: One of the end circles touches the body.

### 3.1. End circle to end circle global self-intersection

Let us consider the plane which contains the end point $\mathbf{C}(0)$ and is perpendicular to $\mathbf{C}'(0)$. If we denote a point on the plane as $\mathbf{x} = (x, y, z)^{\mathrm{T}}$, then the equation of that plane becomes

$$\big(\mathbf{x} - \mathbf{C}(0)\big) \cdot \mathbf{C}'(0) = 0. \tag{7}$$

Similarly the equation of the plane that contains the other end of the pipe is given by

$$\big(\mathbf{x} - \mathbf{C}(1)\big) \cdot \mathbf{C}'(1) = 0. \tag{8}$$

The self-intersection occurs along the intersection of these two planes, see Fig. 1. It also lies on the bisecting plane of the vector $\mathbf{C}(0)\mathbf{C}(1)$. Thus if $\mathbf{x}$ is a self-intersection point, then

$$\left(\mathbf{x} - \frac{\mathbf{C}(0) + \mathbf{C}(1)}{2}\right) \cdot \big(\mathbf{C}(1) - \mathbf{C}(0)\big) = 0. \tag{9}$$

Eqs. (7)–(9) are linear equations and hence, in the case of a regular system the solution is unique. The system becomes singular when the two tangent vectors that attach to both ends of the spine curve lie on the same plane. In such a case there are two possible scenarios. One is that no such radius exists so that the two end circles intersect, and the other is that there are an infinite number of solutions. The latter case happens when the normal planes at the end points lie symmetric with respect to the bisecting plane. In such a case, the minimum radius among the infinite solutions will be the maximum

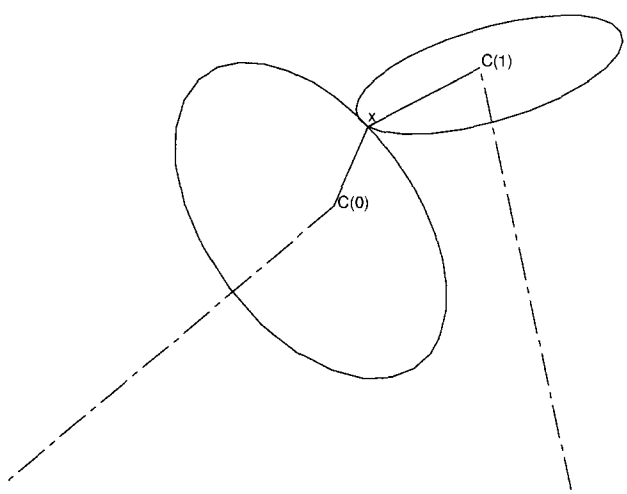


Fig. 1. Two end circles globally self-intersecting at point $\mathbf{x}$.

possible upper limit of the radius such that there will be no end circle to end circle global self-intersection. For further reference we will denote this radius by $r_{ee}$. If there is no such end circle to end circle global self-intersection, we set $r_{ee} = \infty$.

### 3.2. Body to body global self-intersection

The body to body global self-intersection case can be reformulated in terms of two different points on the spine curve that have a minimum distance. This minimum distance should not be understood as the distance between two points whose parameters ($s$ and $t$) are close enough, which amounts to a distance approaching zero, i.e., the trivial solution. Rather, these two points should make the distance function stationary. Therefore, the body to body global self-intersection problem is equivalent to the minimum distance problem.

Non-Uniform Rational B-Spline (NURBS) curves and surface patches are the most popular representation method in CAD/CAM due to their generality, excellent properties and incorporation in international standards such as IGES (Initial Graphics Exchange Specification) and STEP (Standard for the Exchange of Product Model Data). We assume the spine curve can be given by a rational B-spline curve, which can be split into rational Bézier curves by knot insertion. The minimum distance problem can be decomposed into the minimum distance between two points on different curves and the minimum distance between two points on the same curve. The first problem is solved by Zhou et al. (1993), so we focus on the second problem here.

Let the spine curve be given by $\mathbf{C}(t) = (x(t), y(t), z(t))^{\mathrm{T}}$. Assume that the curve is regular, and $\mathbf{C}'(t)$ is continuous.

The squared distance function between two points on the spine curve with parameters $s$ and $t$ is given by

$$\begin{aligned} D(s,t) &= \left|\mathbf{C}(s) - \mathbf{C}(t)\right|^2 \\ &= \big(x(s) - x(t)\big)^2 + \big(y(s) - y(t)\big)^2 + \big(z(s) - z(t)\big)^2. \end{aligned} \tag{10}$$

The stationary points of $D(s,t)$ satisfy the following equations

$$D_s(s,t) = D_t(s,t) = 0 \tag{11}$$

which can be rewritten as

$$\big(\mathbf{C}(s) - \mathbf{C}(t)\big) \cdot \mathbf{C}'(s) = 0, \tag{12}$$

$$\big(\mathbf{C}(s) - \mathbf{C}(t)\big) \cdot \mathbf{C}'(t) = 0. \tag{13}$$

The geometrical interpretation of Eqs. (12) and (13) is that the line connecting the two points $\mathbf{C}(s)$ and $\mathbf{C}(t)$ is *orthogonal* to the spine curve at both points. Without loss of generality we may assume that $\mathbf{C}(t)$ is given as a rational Bézier curve, that is

$$\mathbf{C}(t) = \frac{\sum_{i=0}^{n} w_i \mathbf{P}_i B_{i,n}(t)}{\sum_{i=0}^{n} w_i B_{i,n}(t)} \equiv \frac{\mathbf{r}(t)}{w(t)}. \tag{14}$$

Substituting (14) into (12) gives

$$\left(\frac{\mathbf{r}(s)}{w(s)} - \frac{\mathbf{r}(t)}{w(t)}\right) \cdot \left(\frac{\mathbf{r}'(s)w(s) - \mathbf{r}(s)w'(s)}{w^2(s)}\right) = 0. \tag{15}$$

Multiplying by its own denominator we obtain

$$\big(\mathbf{r}(s)w(t) - \mathbf{r}(t)w(s)\big) \cdot \big(\mathbf{r}'(s)w(s) - \mathbf{r}(s)w'(s)\big) = 0. \tag{16}$$

Similarly Eq. (13) reduces to

$$\big(\mathbf{r}(s)w(t) - \mathbf{r}(t)w(s)\big) \cdot \big(\mathbf{r}'(t)w(t) - \mathbf{r}(t)w'(t)\big) = 0. \tag{17}$$

The first term of the dot product of Eqs. (16) and (17) can be rewritten as

$$\sum_{i=0}^{n}\sum_{j=0}^{n} w_i w_j \mathbf{P}_i \big(B_{i,n}(s)B_{j,n}(t) - B_{j,n}(s)B_{i,n}(t)\big). \tag{18}$$

Since

$$\frac{B_{i,n}(s)B_{j,n}(t) - B_{j,n}(s)B_{i,n}(t)}{s-t} = B_{j,n}(t)\frac{B_{i,n}(s) - B_{i,n}(t)}{s-t} - B_{i,n}(t)\frac{B_{j,n}(s) - B_{j,n}(t)}{s-t}, \tag{19}$$

we can easily factor out $(s-t)$ from the first term of the dot product of Eqs. (16) and (17). Therefore the system of Eqs. (12), (13) for the rational Bézier curve reduces to a system of coupled bivariate polynomial equations with degree $(3n-2)$ in $s$, $(2n-1)$ in $t$ and degree $(2n-1)$ in $s$, $(3n-2)$ in $t$. The system can be robustly and efficiently solved by the Interval Projected Polyhedron algorithm (Sherbrooke and Patrikalakis, 1993; Maekawa and Patrikalakis, 1993; Hu et al., 1996). If we substitute all the solutions computed by the polynomial solver into Eq. (10) and choose the minimum squared distance, then the maximum possible upper limit of the radius $r_{\mathrm{bb}}$ such that body and body of the pipe surface will not globally self-intersect is given by $r_{\mathrm{bb}} = \sqrt{\min_I D(s,t)}/2$, where $I = [0,1] \times [0,1]$ and $D(s,t)$ is the squared distance between two points which make the distance function stationary. If there are no such points, then we set $r_{\mathrm{bb}} = \infty$.

### 3.3. End circle to body global self-intersection

Finally we consider the case of end circle to body global self-intersection. This case can be considered as a special case of body to body global self-intersection. We can substitute $s = 1$ into Eq. (13) which gives

$$\big(\mathbf{C}(1) - \mathbf{C}(t)\big) \cdot \mathbf{C}'(t) = 0. \tag{20}$$

If the spine curve is a rational Bézier curve, Eq. (20) will become a univariate polynomial equation. This equation contains the trivial solution $t = 1$ and therefore $t-1$ can be easily factored out. Similarly, we can substitute $s = 0$ into Eq. (13) and factor out $t$. Notice that the line connecting $\mathbf{C}(t)$ and the end point $\mathbf{C}(1)$ is orthogonal to the spine curve at $\mathbf{C}(t)$ but not necessarily orthogonal at $\mathbf{C}(1)$. Therefore, with the radius equal to half the distance between $\mathbf{C}(t)$ and $\mathbf{C}(1)$, the pipe surface may not self-intersect. In the limiting case of tangential self-intersection, at the intersection point, using the parametrization of Eq. (1), the following equations hold:

$$\mathbf{P}(1,\theta) = \mathbf{P}(t,\phi), \tag{21}$$

$$\mathbf{P}_\theta(1,\theta) \cdot \big(\mathbf{P}_t(t,\phi) \times \mathbf{P}_\phi(t,\phi)\big) = 0. \tag{22}$$

Eq. (22) comes from the fact that the end circle tangentially self-intersects to the body (see Fig. 7). This system consists of four scalar equations with four unknowns, namely $r$, $t$, $\theta$ and $\phi$. We can also form the four scalar equations in terms of polynomials using the rational parametrization of the pipe surface. However we cannot factor out the trivial solution from the system. Maekawa et al. (1997) developed a method to handle such a case. But in this specific case we do not need to use this, as we can easily solve the system using Newton's method, since there is only one solution and we can provide a very accurate initial approximation as follows: We consider a circle at $t = t_m$, i.e., $\mathbf{P}(t_m,\theta)$ using the solution of (20) as $t_m$. By considering this circle as one of the end circles we can use the technique introduced in Section 3.1 to find the intersection point between the two end circles. From this intersection point we can evaluate the radius $r$ and the two angles $\theta$ and $\phi$ for the initial values, using coordinate transformations. In case when the spine curve is planar, we cannot use the technique introduced in Section 3.1 since the linear system becomes singular. In such case we will use the solution of (20) as $t$ and half the distance between $\mathbf{C}(t)$ and $\mathbf{C}(1)$ (or $\mathbf{C}(0)$) as $r$, and $\theta$ and $\phi$ as 0 or $\pi$ as initial approximation. Let us now denote the resulting radius from Newton's solution method by $r_{\mathrm{eb}}$. Also, if there is no such end circle to body global self-intersection, we set $r_{\mathrm{eb}} = \infty$.

### *3.4. A necessary and sufficient condition for nonsingularity*

Using the methods of the previous sections we can now have a necessary and sufficient condition, in terms of the radius $r$, for the nonsingularity of a pipe surface.

We assume that the spine curve is given by $\mathbf{C}(t) = (x(t), y(t), z(t))^{\mathrm{T}}$, $0 \leqslant t \leqslant 1$, and suppose that the curve is regular, and $\mathbf{C}'(t)$ is continuous.

Let $\kappa_{\max}$ be the maximum curvature of the spine curve, and $r_{\mathrm{ee}}$, $r_{\mathrm{bb}}$, $r_{\mathrm{eb}}$ be the maximum possible upper limit radius of the pipe surface such that it does not globally self-intersect between end circle to end circle, body to body and end circle to body of the pipe surface, respectively. Then we have

**Theorem 3.1.** *Let $\mathbf{P}_C(r)$ be the pipe surface with spine curve $\mathbf{C}(t)$ and radius $r$. Then, $\mathbf{P}_C(r)$ is nonsingular if and only if $r < \delta = \min\{1/\kappa_{\max}, r_{\mathrm{ee}}, r_{\mathrm{bb}}, r_{\mathrm{eb}}\}$.*

**Proof.** (if): It is apparent from the discussion on Sections 2, 3.1, 3.2 and 3.3 that if $r < \delta$ then the pipe surface $\mathbf{P}_C(r)$ is nonsingular.

(only if): Suppose now that $\mathbf{P}_C(r)$ is nonsingular. It is enough to show that for all $r \geqslant \delta$, $\mathbf{P}_C(r)$ is singular. But this is obvious since if $r$ is as indicated, the pipe surface will either have a singularity due to local self-intersection or one due to global self-intersection, or both. □

**Remark 3.1.** When the spine curve is planar, Theorem 3.1 can be used to find the maximum offset distance such that the offset of the planar spine curve will not self-intersect.

## 4. Rational parametrizations of pipe surfaces

Lü and Pottmann (1996) showed that any pipe surface with rational spine curve admits a rational parametrization. They represent the pipe surface as

$$\mathbf{P}(u,t) = \mathbf{C}(t) + r\mathbf{N}(u,t), \tag{23}$$

where for each fixed $t$, $\mathbf{N}(u,t)$ is the unit circle with center $\mathbf{C}(t)$ in the normal plane $\mathbf{C}'(t)\cdot\mathbf{x} = 0$ of the spine curve. The key problem in the method they developed is the decomposition of a nonnegative rational polynomial function into a sum of squares of two rational functions. In this section we develop an algorithmic solution of this problem. The problem is as follows:

**Problem 4.1.** Given the (rational) spine curve $\mathbf{C}(t)$ of degree $(n+1)$, find (rational) functions $\alpha(t)$ and $\beta(t)$ such that

$$\left|\mathbf{C}'(t)\right|^2 = \alpha^2(t) + \beta^2(t). \tag{24}$$

First, we shall prove that such a decomposition always exists which satisfies the condition that $\alpha(t)$ is at least one degree higher than $\beta(t)$. We will only prove this for the integral case since the rational case can be derived by dividing the integral solutions by $w(t)$.

Let $f(t) \in \mathbb{R}[t]$ be a polynomial of positive degree satisfying the following:

$$f(t) = a_n t^n + a_{n-1}t^{n-1} + \cdots + a_1 t + a_0 \geqslant 0, \quad \text{for all } t \in \mathbb{R}. \tag{25}$$

Then, it is well known that $a_n > 0$ and $n$ is an even integer. We may factor $f(t)$ as follows:

$$\begin{aligned} f(t) = a_n(t-\sigma_1)^{k_1}(t-\sigma_2)^{k_2}\cdots(t-\sigma_p)^{k_p}\left(t^2-(\tau_1+\bar{\tau}_1)t+\tau_1\bar{\tau}_1\right)^{m_1}\cdots \\ \left(t^2-(\tau_q+\bar{\tau}_q)t+\tau_q\bar{\tau}_q\right)^{m_q}, \end{aligned} \tag{26}$$

where $\sigma_i$ $(i = 1,\ldots,p)$ are the real roots of $f(t)$ with multiplicities $k_i$ $(i = 1,\ldots,p)$ and $\tau_j, \bar{\tau}_j$ $(j = 1,\ldots,q)$ are the pairs of conjugate complex roots of $f(t)$ with multiplicities $m_j$ $(j = 1,\ldots,q)$, respectively. Adding up the degrees of the two sides of the above equation we see that

$$n = k_1 + k_2 + \cdots + k_p + 2(m_1 + m_2 + \cdots + m_q). \tag{27}$$

Further, notice that $k_1, k_2, \ldots, k_p$ are all even, since $f(t) \geqslant 0$ for all $t \in \mathbb{R}$.

Let

$$g(t) = \left[(t-\sigma_1)^{k_1/2}(t-\sigma_2)^{k_2/2}\cdots(t-\sigma_p)^{k_p/2}\right]g_1(t), \tag{28}$$

where $g_1(t)$ comes from extracting all the squared factors from the term

$$\left(t^2-(\tau_1+\bar{\tau}_1)t+\tau_1\bar{\tau}_1\right)^{m_1}\cdots\left(t^2-(\tau_q+\bar{\tau}_q)t+\tau_q\bar{\tau}_q\right)^{m_q}.$$

Let

$$\omega_i(t) = t^2-(\tau_i+\bar{\tau}_i)t+\tau_i\bar{\tau}_i = (t-\psi_i)^2+\phi_i^2, \tag{29}$$

where without loss of generality $\psi_i = (\tau_i + \bar{\tau}_i)/2$, and $\phi_i = \sqrt{(\tau_i\bar{\tau}_i - \psi_i^2)}$, then $f(t)$ can be written in the form

$$f(t) = a_n g^2(t)\omega_1(t)\cdots\omega_m(t). \quad \text{with } m \leqslant q. \tag{30}$$

We prove by induction on $m$ the existence of $\alpha(t)$ and $\beta(t)$ such that $f(t) = \alpha^2(t) + \beta^2(t)$ with $\alpha(t)$ at least one degree higher than $\beta(t)$:

(1) If $m = 0$, then

$$\alpha(t) = \sqrt{a_n}g(t), \qquad \beta(t) = 0. \tag{31}$$

(2) If $m = 1$ then

$$\begin{aligned} f(t) &= a_n g^2(t)\big((t-\psi_1)^2 + \phi_1^2\big) \\ &= \big(\sqrt{a_n}g(t)(t-\psi_1)\big)^2 + \big(\sqrt{a_n}g(t)\phi_1\big)^2 \\ &= \alpha^2(t) + \beta^2(t) \end{aligned} \tag{32}$$

and $\alpha(t)$ is exactly one degree higher than $\beta(t)$.

(3) If $k+1 \geqslant 1$ terms of $\omega_i(t)$ are left after extracting the squared term from $f(t)$, we assume that

$$\omega_1(t)\cdots\omega_k(t) = h_1^2(t) + h_2^2(t) \tag{33}$$

with $h_1(t)$ at least one degree higher than $h_2(t)$, then

$$\begin{aligned} \omega_1(t)\cdots\omega_k(t)\omega_{k+1}(t) &= \big(h_1^2(t) + h_2^2(t)\big)\cdot\big((t-\psi_{k+1})^2 + \phi_{k+1}^2\big) \\ &= \big((t-\psi_{k+1})h_1(t) + \phi_{k+1}h_2(t)\big)^2 \\ &\quad + \big((t-\psi_{k+1})h_2(t) - \phi_{k+1}h_1(t)\big)^2 \end{aligned} \tag{34}$$

and

$$f(t) = \alpha^2(t) + \beta^2(t), \tag{35}$$

where

$$\begin{aligned} \alpha(t) &= \sqrt{a_n}g(t)\big((t-\psi_{k+1})h_1(t) + \phi_{k+1}h_2(t)\big), \\ \beta(t) &= \sqrt{a_n}g(t)\big((t-\psi_{k+1})h_2(t) - \phi_{k+1}h_1(t)\big). \end{aligned} \tag{36}$$

The proof is now complete. Note, however, that the expressions of $\alpha(t)$ and $\beta(t)$ are not unique because we can also decompose $\omega_i(t)$ as

$$\begin{aligned} \omega_i(t) &= t^2 - 2\psi_i t + \psi_i^2 + \phi_i^2 \\ &= \left(\sqrt{\psi_i^2 + \phi_i^2}\left(1 - \frac{\psi_i t}{\psi_i^2 + \phi_i^2}\right)\right)^2 + \left(\frac{\phi_i t}{\sqrt{\psi_i^2 + \phi_i^2}}\right)^2. \end{aligned} \tag{37}$$

**Remark 4.1.** Let $f(t)$ be as in (25), and let $a(t), b(t)$ be real polynomials so that

$$f(t) = a^2(t) + b^2(t) \tag{38}$$

then, there is an infinite number of polynomial pairs $(A(t), B(t))$ that also satisfy Eq. (38).

**Proof.** Take a real number $c$ so that $-1 \leqslant c \leqslant 1$, and consider

$$A(t) = ca(t) + \sqrt{1-c^2}b(t), \qquad B(t) = -\sqrt{1-c^2}a(t) + cb(t). \tag{39}$$

Note that $A(t), B(t)$ satisfy (38). Since there is an infinite number of $c$'s to choose from, it follows that there is an infinite number of polynomial pairs that satisfy Eq. (38). □

Therefore, the key problem in finding (rational) functions $\alpha(t)$ and $\beta(t)$ is to solve all the complex roots of the equation (Lü and Pottmann, 1996)

$$\left|\mathbf{C}'(t)\right|^2 = a_{2n}t^{2n} + a_{2n-1}t^{2n-1} + \cdots + a_0 = 0. \tag{40}$$

Let $t = \psi + \mathrm{i}\phi$, then Eq. (40) is equivalent to the following set of two nonlinear equations:

$$\begin{aligned}
&a_{2n}\left(\psi^{2n} - \binom{2n}{2}\psi^{2n-2}\phi^2 + \cdots + (-1)^n\phi^{2n}\right)\\
&\quad + a_{2n-1}\left(\psi^{2n-1} - \cdots + (-1)^{n-1}\binom{2n-1}{2n-2}\psi\phi^{2n-2}\right) + \cdots + a_0 = 0,\\
&a_{2n}\left(\binom{2n}{1}\psi^{2n-1}\phi - \cdots + (-1)^{n-1}\binom{2n}{2n-1}\psi\phi^{2n-1}\right)\\
&\quad + a_{2n-1}\left(\binom{2n-1}{1}\psi^{2n-2}\phi - \cdots + (-1)^{n-1}\phi^{2n-1}\right) + \cdots + a_1\phi = 0.
\end{aligned} \tag{41}$$

This set of two nonlinear polynomial equations with two unknowns $(\psi, \phi)$ can be solved by the Interval Projected Polyhedron Algorithm (Sherbrooke and Patrikalakis, 1993; Maekawa and Patrikalakis, 1993; Hu et al., 1996). After obtaining all the complex roots of Eq. (40) we can form $\alpha(t)$ and $\beta(t)$ according to Eqs. (32), (33) and (34). We can construct another group of solutions of Eq. (24) by simply interchanging $\alpha(t)$ with $\beta(t)$.

A typical plot of parameter $u$ versus arc length $s$ along half of the unit circle $\mathbf{N}(u,t)$ (see Eq. (23)) is shown in Fig. 2 with a solid line. It is clear from the figure that the curve does not have constant parametric speed. Also $u$ must vary from 0 to $\infty$ to complete the half circle. Such variation is obviously inappropriate for implementation in the computer. To improve the parametrization we introduce a rational bilinear transformation (Tiller, 1983) of the form

$$u = \frac{v}{c(1-v)}, \quad 0 \leqslant v \leqslant 1, \tag{42}$$

where $c$ is a positive constant. The dashed line in Fig. 2 shows the improved parametrization, which has nearly constant parametric speed, a feature important in many applications. Note that the denominator $(1-v)$ will cancel out when Eq. (42) is substituted into $\mathbf{N}(u,t)$ of Eq. (23). To obtain the other half of the circle we just replace $c$ by $-c$ in Eq. (42).

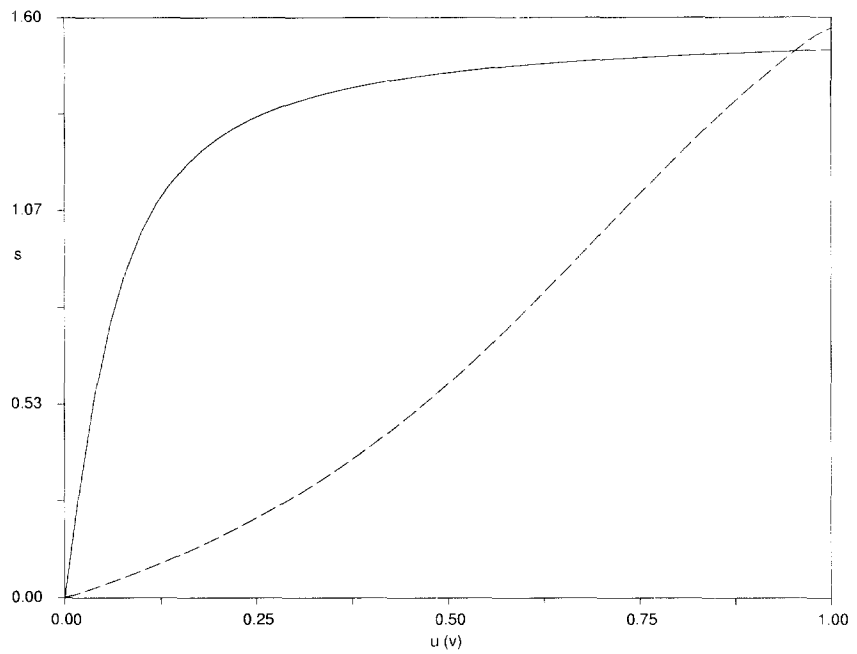


Fig. 2. Parameter $u$ or $v$ versus arc length $s$ along half of the unit circle $\mathbf{N}(u,t)$, with $c = 24$.

## 5. Examples

### 5.1. Local self-intersection

The parabola $y = x^2$ has its largest curvature $\kappa = 2$ at $(0,0)$. Therefore in order to have no local self-intersection the radius should be $r < 1/2$. Fig. 3 shows the local self-intersection of the pipe surface with parabolic spine with radius 0.8. Obviously, there is a local self-intersection on the pipe surface corresponding to the point (0, 0) at the spine curve.

### 5.2. End circle to end circle global self-intersection

Fig. 4 illustrates the case when end circles are touching each other. The control points of the spine curve, which is a cubic integral Bézier curve, are given by (2.9, 3.0, 4.1), (0.0, 1.0, 2.0), (5.0, −2.0, 1.0) and (3.0, 3.1, 4.0). The linear system (7), (8), (9) gives us the intersection point as (2.918, 3.055, 4.023) with radius $r = 0.0963$.

### 5.3. Body to body global self-intersection

Figs. 5 show two different views of the minimum distance between the points on a rational Bézier curve of degree 4. The solid squares indicate the five control points (−0.3, 0.8, 0.1), (0.3, 0.15, −0.45), (0, 0, 0.2), (−0.2, 0.1, 0.8), (0.3, 0.8, −0.6) with weights

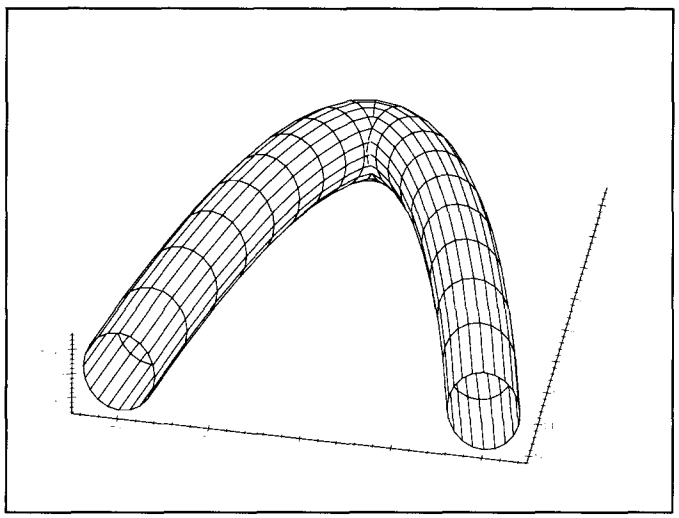

Fig. 3. Local self-intersection ($r = 0.8$).

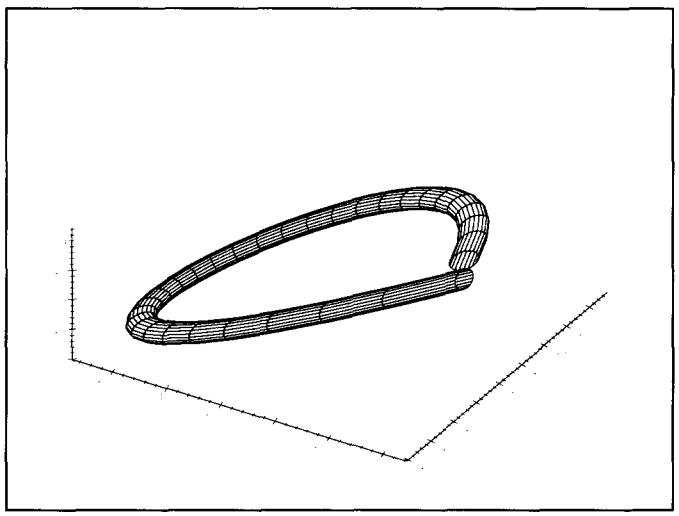

Fig. 4. End circle to end circle global self-intersection ($r = 0.0963$).

1, 2, 0.5, 3, 1. The minimum distance between two points on the spine curve can be obtained as 0.157556, which is between the points of the parameters ($t = 0.102506$) and ($s = 0.952132$). The spine curve has a global maximum curvature at $t = 0.70618$ with curvature value $\kappa = 48.7601$. Therefore the pipe surface starts to self-intersect locally when $r = 0.0205$ and globally when $r = 0.078778$. The situation when $r = 0.078778$ is shown in Fig. 6 where two different parts of the body of the pipe surface touch each other and locally self-intersect.

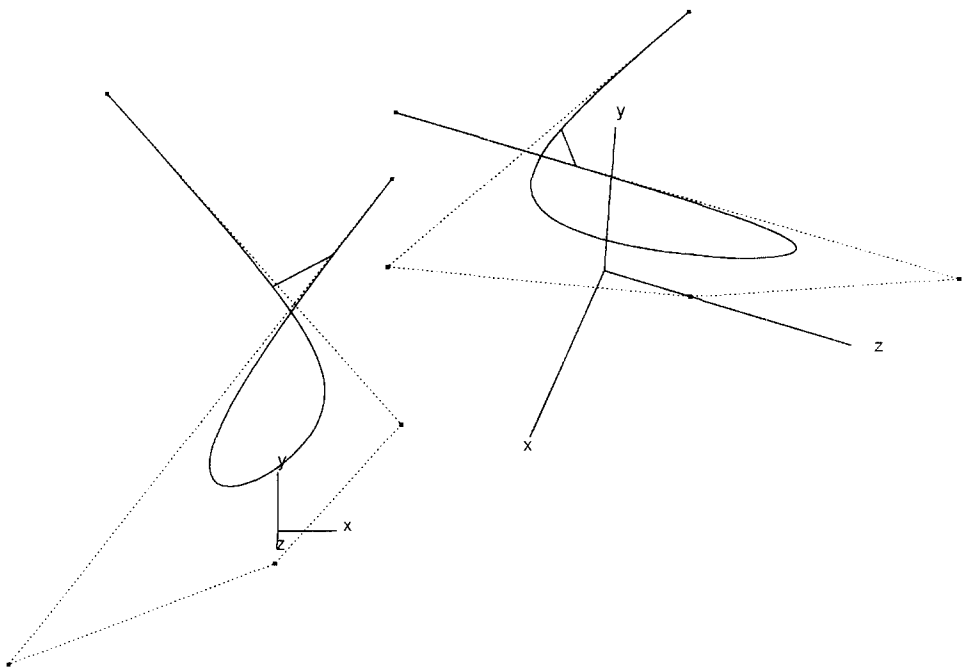


Fig. 5. Two different views of spine curve which has minimum distance between two interior points.

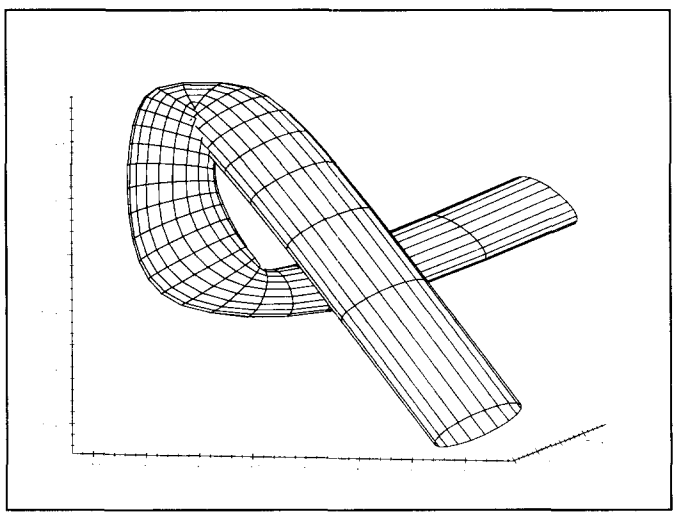

Fig. 6. Body to body tangential intersection and local self-intersection ($r = 0.078778$).

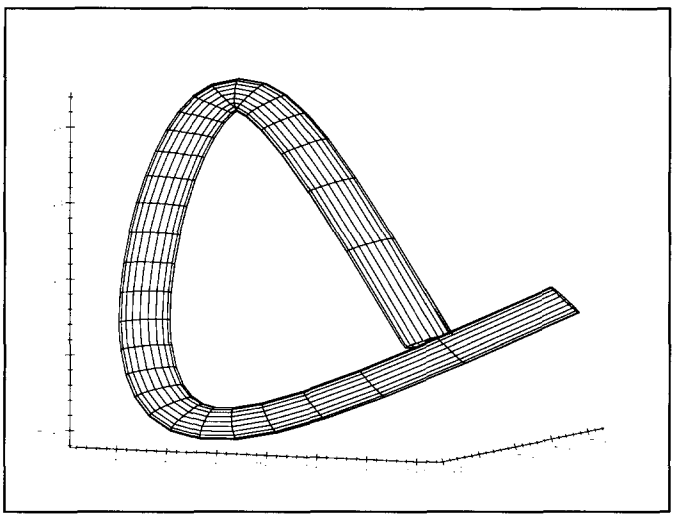

Fig. 7. End circle to body tangential global and local self-intersections ($r = 0.078778$).

### 5.4. End circle to body global self-intersection—3D spine curve

The spine curve with control points $(-0.3, 0.8, 0.1)$, $(0.24, 0.15, -0.45)$, $(0,0,0.2)$, $(-0.24, 0.12, 0.96)$ and $(-2, 0.6, 0)$ and weights 1, 2, 0.5, 2.5, 1 respectively, has minimum distance 0.0595918 between two points $t = 0.0370295$ and $t = 1$. However with $r = 0.0595918/2 = 0.0297959$, the pipe surface does not self-intersect, since the vector $\mathbf{C}(1) - \mathbf{C}(0.0370295)$ is not orthogonal to the spine curve at $t = 1$. With the help of Newton's method we obtain the touching radius as $r = 0.041829$. The spine curve also has a global maximum curvature at $t = 0.761006$ with $\kappa = 31.272916$. Therefore the pipe surface starts to self-intersect locally when $r = 0.031977$ and globally when $r = 0.041829$. Fig. 7 shows the pipe surface with $r = 0.041829$.

### 5.5. End circle to body global self-intersection—2D spine curve

The spine curve with control points $(-0.3, 0.8, 0)$, $(0.6, 0.3, 0)$, $(0,0,0)$, $(-0.3, 0.2, 0)$ and $(-0.15, 0.6, 0)$ and weights 1, 1, 2, 3, 1 respectively, has minimum distance 0.0777421 between two points $t = 0.0658996$ and $t = 1$. By using Newton's method we obtain the touching radius as $r = 0.055754$. This distance is the maximum offset distance such that the offset of the planar spine curve will not self-interset. Fig. 8 shows the offset curves when $r = 0.055754$.

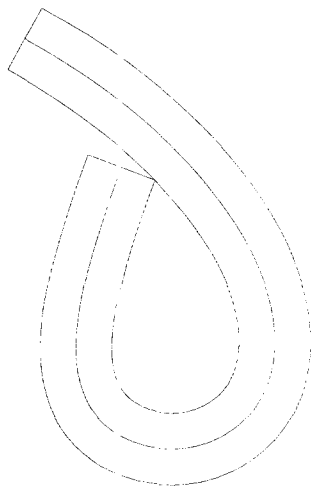

Fig. 8. Offset curves of the planar spine curve ($r = 0.055754$).

### 5.6. Rationalization

#### 5.6.1. Example 1

The spine curve $\mathbf{C}(t)$ of a pipe surface is an integral cubic Bézier curve with control points (2.0, −3.0, 0.0), (4.0, 1.5, 2.0), (7.0, 4.0, 4.0), (10.0, 2.0, 6.0). Then

$$\left|\mathbf{C}'(t)\right|^2 = 65.25t^4 + 144.0t^3 - 58.5t^2 - 252.0t + 245.25. \tag{43}$$

The four complex roots of $|\mathbf{C}'(t)|^2 = 0$ are found by the Interval Projected Polyhedron solver; they are:

$$t = \psi_1 \pm \phi_1 \mathrm{i} = 0.80641507 \pm 0.44897328\mathrm{i},$$
$$t = \psi_2 \pm \phi_2 \mathrm{i} = -1.90986334 \pm 0.87439026\mathrm{i}.$$

Based on the complex roots of $|\mathbf{C}'(t)|^2 = 0$, we obtain $\omega_1(t)$ and $\omega_2(t)$ according to Eq. (29). Now $|\mathbf{C}'(t)|^2$ can be rewritten in the format of $f(t)$ in Eq. (30), with $a_n = a_4 = 65.25$, $g(t) = 1$, and $m = 2$. Then we follow the induction steps of Eqs. (32)–(36) and obtain four solutions of $\alpha(t)$ and $\beta(t)$. They are:

(1)

$$\alpha(t) = 8.07774721t^2 + 8.91337619t - 15.61202716,$$
$$\beta(t) = 10.68979614t + 1.23069427.$$

The pipe surface rationalized with the above $\alpha(t)$ and $\beta(t)$ with $r = 0.5$ and

$$u = \frac{v}{\pm 24(1-v)}, \quad v \in [0,\ 1]$$

is shown in Fig. 9. The resulting rational pipe surface is of degree 15 in $t$.

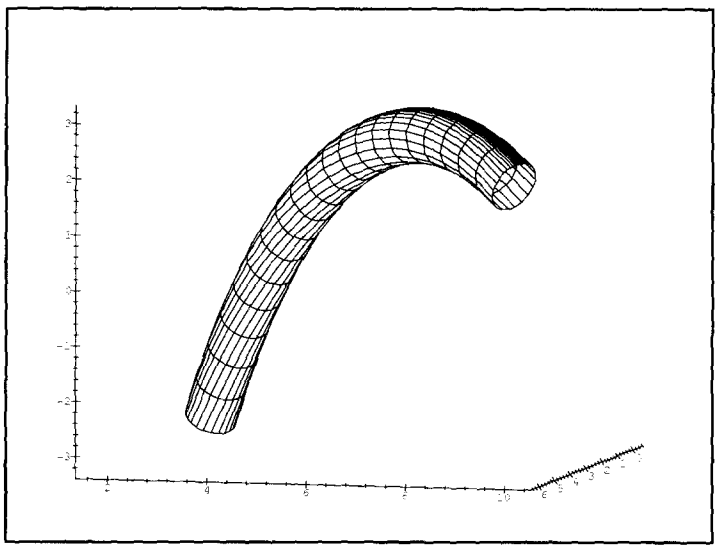

Fig. 9. A rational pipe surface with $r = 0.5$, $\alpha(t) = 8.07774721t^2 + 8.91337619t - 15.61202716$, $\beta(t) = 10.68979614t + 1.23069427$.

(2)

$$\alpha(t) = 10.68979614t + 1.23069427,$$
$$\beta(t) = 8.07774721t^2 + 8.91337619t - 15.61202716,$$

(3)

$$\alpha(t) = 8.07774721t^2 + 8.91337619t - 9.26973768,$$
$$\beta(t) = 3.43641082t - 12.62228045,$$

(4)

$$\alpha(t) = 3.43641082t - 12.62228045,$$
$$\beta(t) = 8.07774721t^2 + 8.91337619t - 9.26973768.$$

The pipe surface rationalized with above $\alpha(t)$ and $\beta(t)$ with $r = 0.5$ and

$$u = \frac{v}{\pm 16(1-v)}, \quad v \in [0,\ 1]$$

is shown in Fig. 10. The resulting rational pipe surface is of degree 15 in $t$.

*5.6.2. Example 2*

The spine curve $\mathbf{C}(t)$ of a pipe surface is an integral Bézier curve of degree 4 with control points (2.0, −3.0, 0.0), (4.0, 1.5, 2.0), (7.0, 4.0, 4.0), (10.0, 2.0, 6.0), (15.0, 3.0, 10.0). Then

$$\left|\mathbf{C}'(t)\right|^2 = 1808t^6 - 2688t^5 - 588t^4 + 2912t^3 - 552t^2 - 672t + 452. \tag{44}$$

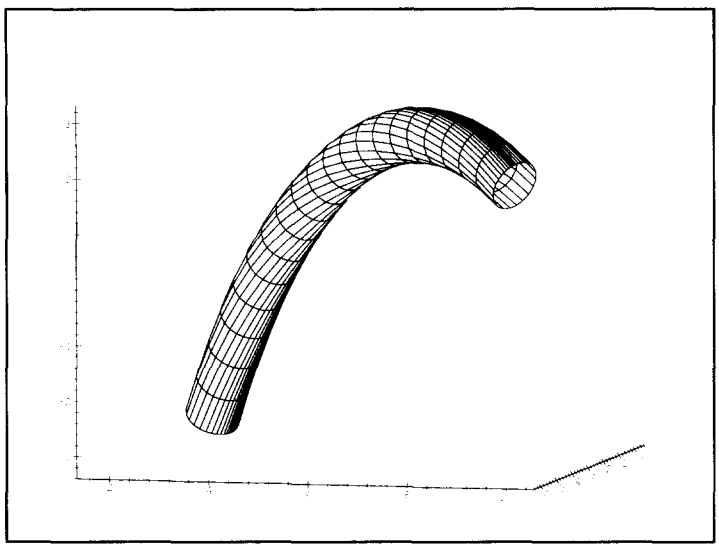

Fig. 10. A rational pipe surface with $r = 0.5$, $\alpha(t) = 3.43641082t - 12.62228045$, $\beta(t) = 8.07774721t^2 + 8.91337619t - 9.26973768$.

The six complex roots of $|\mathbf{C}'(t)|^2 = 0$ are found by the Interval Projected Polyhedron solver, which are:

$$t = \psi_1 \pm \phi_1 \mathrm{i} = 1.06394917 \pm 0.49424887\mathrm{i},$$

$$t = \psi_2 \pm \phi_2 \mathrm{i} = 0.41517999 \pm 0.38919525\mathrm{i},$$

$$t = \psi_3 \pm \phi_3 \mathrm{i} = -0.73576633 \pm 0.13986292\mathrm{i}.$$

Based on the complex roots of $|\mathbf{C}'(t)|^2 = 0$, four solutions of $\alpha(t)$ and $\beta(t)$ are obtained according to Eqs. (29), (30),(32)–(36). They are:

(1)

$$\alpha(t) = 42.52058324t^3 - 31.60822109t^2 - 30.41757826t + 4.11870005,$$

$$\beta(t) = 31.61750631t^2 + 10.10278671t - 20.85752419.$$

The pipe surface rationalized with the above $\alpha(t)$ and $\beta(t)$ with $r = 0.5$ and

$$u = \frac{v}{\pm 24(1 - v)}, \quad v \in [0,\ 1]$$

is shown in Fig. 11. The resulting pipe surface is of degree 22 in $t$.

(2)

$$\alpha(t) = 42.52058324t^3 - 31.60822109t^2 - 19.93776632t + 18.59540154,$$

$$\beta(t) = 10.41399412t^2 + 3.37193818t + 10.30587440.$$

(3)

$$\alpha(t) = 42.52058324t^3 - 31.60822109t^2 - 40.92535616t + 11.48455572,$$

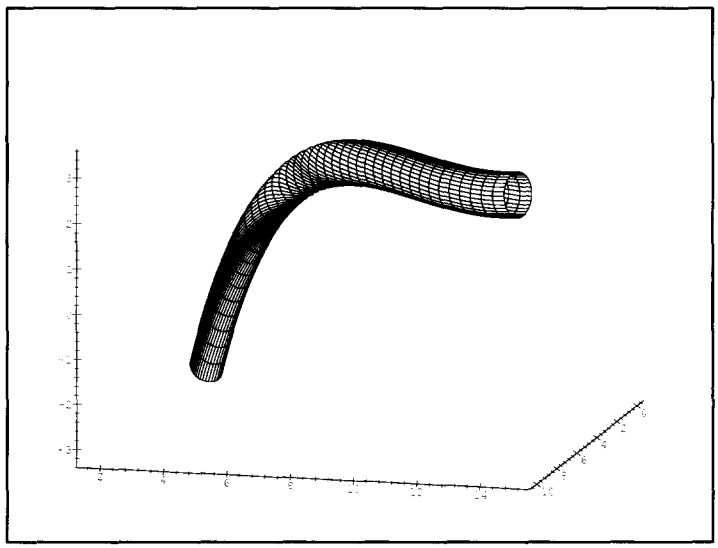

Fig. 11. A rational pipe surface with $r = 0.5$, $\alpha(t) = 42.52058324t^3 - 31.60822109t^2 - 30.41757826t + 4.11870005$, $\beta(t) = 31.61750631t^2 + 10.10278671t - 20.85752419$.

$$\beta(t) = 43.51161216t^2 - 7.49013210t - 17.89147801,$$

(4)

$$\alpha(t) = 42.52058324t^3 - 31.60822109t^2 - 18.68824745t + 21.07986286,$$
$$\beta(t) = 1.48011174t^2 - 20.96485700t - 2.76394416.$$

The pipe surface rationalized with above $\alpha(t)$ and $\beta(t)$ with $r = 0.5$ and

$$u = \frac{v}{\pm 24(1-v)}, \quad v \in [0,\ 1]$$

is shown in Fig. 12. The resulting pipe surface is of degree 22 in $t$.

If we denote the parameter along the circumferential direction by $u$, it is clear from Figs. 9 to 12 that the isoparametric lines ($u$ = constant) usually twist along the pipe. If we construct Finite Element meshes, using for example, a mapped mesh generator, less twist of the isoparametric lines makes the meshes more suitable for FE analysis. We use the integral of the square of the torsion of the isoparametric lines ($u$ = constant) as the standard to distinguish between better and worse parametrization.

For the parametrization shown in Fig. 11,

$$\int_{-\infty}^{\infty} \left( \int_0^1 \tau^2(t,u)\,\mathrm{d}t \right) \mathrm{d}u = 1.465215, \tag{45}$$

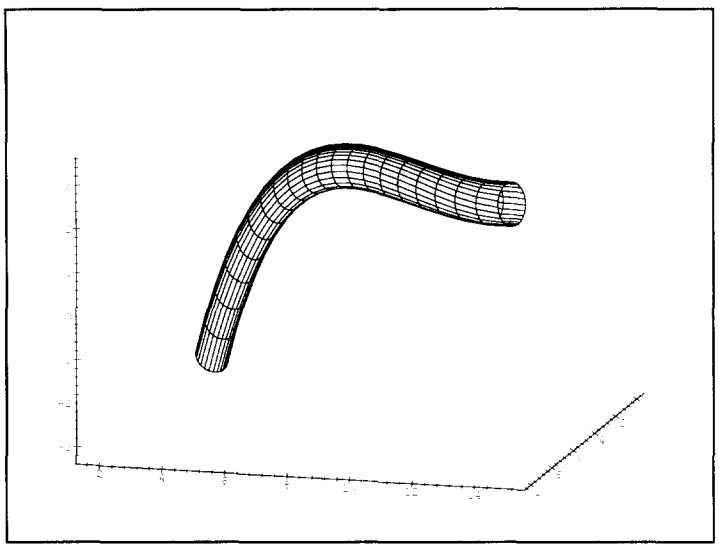

Fig. 12. A rational pipe surface with $r = 0.5$, $\alpha(t) = 42.52058324t^3 - 31.60822109t^2 - 18.68824745t + 21.07986286$, $\beta(t) = 1.48011174t^2 - 20.96485700t - 2.76394416$.

while for the parametrization shown in Fig. 12,

$$\int_{-\infty}^{\infty} \left( \int_0^1 \tau^2(t,u)\,\mathrm{d}t \right) \mathrm{d}u = 0.065176, \tag{46}$$

Therefore, the parametrization shown in Fig. 12 is better than that shown in Fig. 11.

## 6. Reliable approximation of a space curve

Cho et al. (1996) have presented a method for approximating a set of mutually non-intersecting simple space Bézier curves within a prescribed tolerance using a piecewise linear curve. In addition, the existence of a homeomorphism between the curve and its approximant has been ensured. However, the latter does not guarantee that the curve and its approximant are the same topological 'objects' within the space; See Fig. 13 for an example. Here the original curve does not have knots, while the piecewise linear approximation is knotted. The reason for this is the possible presence of knots in space curves. As an example, let us consider a simple closed knotted curve $\mathbf{C}_k$ and the usual circle $\mathbf{C} = \{(x,y,z) \mid x^2+y^2 = 1, z = 0\}$. Then, it is a fact that there exists a homeomorphism $h : \mathbf{C}_k \to \mathbf{C}$, between $\mathbf{C}_k$ and $\mathbf{C}$, but there is no (space) homeomorphism

$$f : \mathbb{R}^3 \to \mathbb{R}^3$$

that maps $\mathbf{C}_k$ onto $\mathbf{C}$. In other words, no matter how hard we try, we cannot untie the knot in $\mathbf{C}_k$—within the space $\mathbb{R}^3$—and make $\mathbf{C}_k$ look exactly like the circle $\mathbf{C}$. (in terms

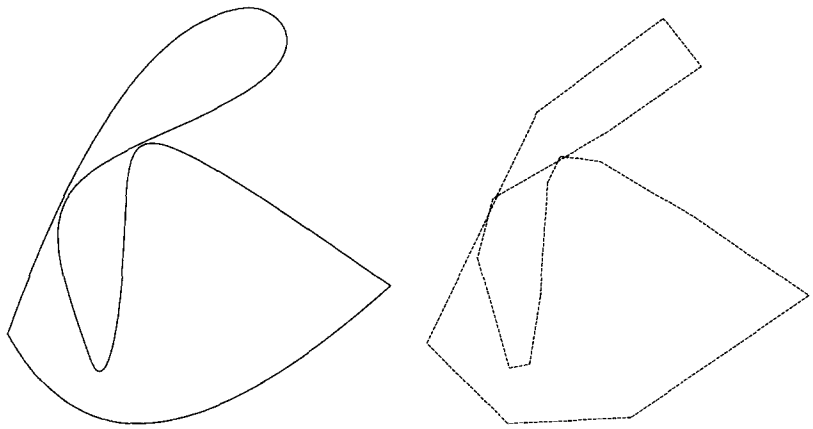

Fig. 13. A composite space curve (solid line) without knots and its knotted approximation (dashed line), see (Peters, 1997).

of *homotopy*, the spaces $\{\mathbb{R}^3 - \mathbf{C}_k\}$ and $\{\mathbb{R}^3 - \mathbf{C}\}$, do not have the same fundamental groups (Moise, 1997, p. 103, Theorem 1)).

The above example shows that if one wants to approximate a space curve with another curve and at the same time wants to ensure not only that the two curves are homeomorphic, but *space homeomorphic*, he would then have to resort to the broader notion of space (or ambient) homeomorphism.

**Definition 6.1.** Let $A, B$ be subsets of $\mathbb{R}^3$. Then we say that $A$ and $B$ are space (ambiently) homeomorphic if there exists a homeomorphism

$$H : \mathbb{R}^3 \to \mathbb{R}^3$$

that maps $A$ onto $B$.

In the special case where $A$ and $B$ are the simple space curves $\mathbf{C}_1$ and $\mathbf{C}_2$, we in addition say that $\mathbf{C}_1$ and $\mathbf{C}_2$ have the same *knot* type.

In this section we will apply the idea of the pipe surface to find a topologically reliable piecewise linear approximation of a given nonsingular space curve $\mathbf{C}(t)$. More precisely, we will deal with the following problem:

**Problem 6.1.** Given the regular rational space curve $\mathbf{C}(t)$, $0 \leqslant t \leqslant 1$, find a piecewise linear curve $\mathbf{K}(t)$ so that

(1) $\mathbf{K}(t)$ approximates $\mathbf{C}(t)$ within a specified tolerance, and
(2) $\mathbf{K}(t)$ and $\mathbf{C}(t)$ are ambiently homeomorphic.

We present a solution to the above problem that is based on the following construction. Let the positive number $r$ be such that the pipe surface $\mathbf{P}_C(r)$ is nonsingular. We can then represent $\mathbf{P}_C(r)$ as in (23),

$$\mathbf{P}_C(r)(u,t) = \mathbf{C}(t) + r\,\mathbf{N}(u,t).$$

Using the techniques of (Cho et al., 1996), we then construct a piecewise linear curve $\mathbf{K}(t)$ so that the following are satisfied:

- $\mathbf{K}(t)$ lies inside $\mathbf{P}_C(r)$,
- For every $t$, the unit disk $\overline{N(u,t)}$ intersects $\mathbf{K}(t)$ at precisely one point, and
- $\mathbf{K}(0) = \mathbf{C}(0)$, $\mathbf{K}(1) = \mathbf{C}(1)$.

Roughly speaking, the curve $\mathbf{K}(t)$ looks *exactly* like the spine curve $\mathbf{C}(t)$ *inside* the pipe surface $\mathbf{P}_C(r)$. We will now show that if $\mathbf{K}(t)$ is as above, then $\mathbf{C}(t)$ and $\mathbf{K}(t)$ are indeed *ambiently* homeomorphic. Note first that the condition of the second bullet above, implies that $\mathbf{K}(t)$ has no knots *within* the pipe $\mathbf{P}_C(r)$. In addition, the two curves $\mathbf{K}(t)$ and $\mathbf{C}(t)$ have the same tubular neighborhood, namely the interior $P^i = \mathrm{Int}(\mathbf{P}_C(r))$, of the pipe surface. Thus, by a continuous sliding we may move $\mathbf{K}(t)$ onto $\mathbf{C}(t)$. The latter implies that there is an isotopy

$$H : [0,1] \times P^i \to P^i \tag{47}$$

with the property

(1) $h_t(x) = H(t,x) : P^i \to P^i$ is a homeomorphism, for all $t$,
(2) $H(0,x) = x$, and
(3) The map $H(1,x)$ maps $\mathbf{C}(t)$ onto $\mathbf{K}(t)$.

Finally, since the boundary of interior of the pipe $\mathbf{P}_C(r)$ is a 2-sphere, we may extend the homeomorphism $H(1,x)$ onto the whole space $\mathbb{R}^3$.

## 7. Concluding remarks

In this paper we have attempted a theoretical analysis on the question of nonsingularity of pipe surfaces with rational spine curve. This analysis can be applied to finding a topologically reliable approximation of a space curve as mentioned in Section 6. Also as indicated in Remark 3.1, this can be used for selecting a maximum possible tool size such that the cutter will not overcut the part in 2.5D pocket machining.

In addition we developed algorithms for the rational parametrization of such surfaces. It is apparent from Section 4 that for a given pipe surface $\mathbf{P}_C(r)$ there are many available parametrizations of the surface. It would be useful to investigate which of these parametrizations is 'better' in terms of specific applications.

It has also been mentioned that pipe surfaces are useful theoretical tools. Do Carmo (1976) uses nonsingular pipe surfaces in the proof of two very important theorems in Differential Geometry concerning the total curvature of space curves, namely Fenchel's theorem and the Fary–Milnor theorem. One of the fundamental problems in Knot theory is to find necessary and sufficient conditions for a closed simple space curve to be *knotted*. The theorem of Fary–Milnor gives such a sufficient condition. We hope that by investigating the (nonsingular) pipe surface whose spine curve is a rational simple and *closed* space curve one can develop such a (relatively) simple condition.

## Acknowledgements

Funding for this work was obtained, in part, from the Office of Naval Research under grant number N00014-96-1-0857. The authors would like to thank Mr. S.L. Abrams for his assistance, Prof. T.J. Peters for his comments and the referees for their suggestions which improved the paper.

## References

Cho, W., Maekawa, T. and Patrikalakis, N.M. (1996), Topologically reliable approximation of composite Bézier curves, Computer Aided Geometric Design 13, 497–520.

do Carmo, P.M. (1976), *Differential Geometry of Curves and Surfaces*, Prentice-Hall, Englewood Cliffs, NJ.

Farouki, R.T. and Sverrisson, R. (1996), Approximation of rolling-ball blends for free-form parametric surfaces, Computer-Aided Design 28, 871–878.

Hoschek, J. and Lasser, D. (1993), *Fundamentals of Computer Aided Geometric Design*, A K Peters, Wellesley, MA, 1993 (Translated by L.L. Schumaker).

Hu, C.-Y., Maekawa, T., Sherbrooke, E.C. and Patrikalakis, N.M. (1996), Robust interval algorithm for curve intersections, Computer-Aided Design 28, 495–506.

Kreyszig, E. (1959), *Differential Geometry*, University of Toronto Press, Toronto.

Lü, W. and Pottmann, H. (1996), Pipe surfaces with rational spine curve are rational, Computer Aided Geometric Design 13, 621–628.

Maekawa, T., Cho, W. and Patrikalakis, N.M. (1997), Computation of self-intersections of offsets of Bézier surface patches, Journal of Mechanical Design, ASME Transactions 119, 275–283.

Maekawa, T. and Patrikalakis, N.M. (1993), Computation of singularities and intersections of offsets of planar curves, Computer Aided Geometric Design 10, 407–429.

Moise, E.E. (1997), *Geometric Topology in Dimensions* 2 *and* 3, Graduate Texts in Mathematics, Springer, New York.

Monge, G. (1850), *Application de l'Analyse à la Géométrie*, Bachelier, Paris.

Pegna, J. and Wilde, D.J. (1990), Spherical and circular blending of functional surfaces, Journal of OMAE, Transactions of the ASME 112, 134–142.

Peters, T.J. (1997), personal communication.

Rossignac, J.R. (1985), Blending and offseting solid models, PhD thesis, University of Rochester, Production Automation Project Technical Memorandum No. 54.

Shani, U. and Ballard, D.H. (1984), Splines as embeddings for generalized cylinders, Computer Vision, Graphics and Image Processing 27, 129–156.

Sherbrooke, E.C. and Patrikalakis, N.M. (1993), Computation of the solutions of nonlinear polynomial systems, Computer Aided Geometric Design 10, 379–405.

Tiller, W. (1983) Rational B-splines for curve and surface representation, IEEE Computer Graphics and Applications 3, 61–69.

Leu Wang, L., M. C., and Blackmore, D. (1997), Generating sweep solids for NC verification using the SEDE method, in: *Proceedings of the Fourth Symposium on Solid Modeling and Applications*, Atlanta, Georgia, May 14–16, 364–375.

Zhou, J., Sherbrooke, E.C. and Patrikalakis, N.M. (1993), Computation of stationary points of distance functions, Engineering with Computers 9, 231–246.